iScience

CellPress
OPEN ACCESS

Article

Pretrial predictors of conflict response efficacy in the human prefrontal cortex

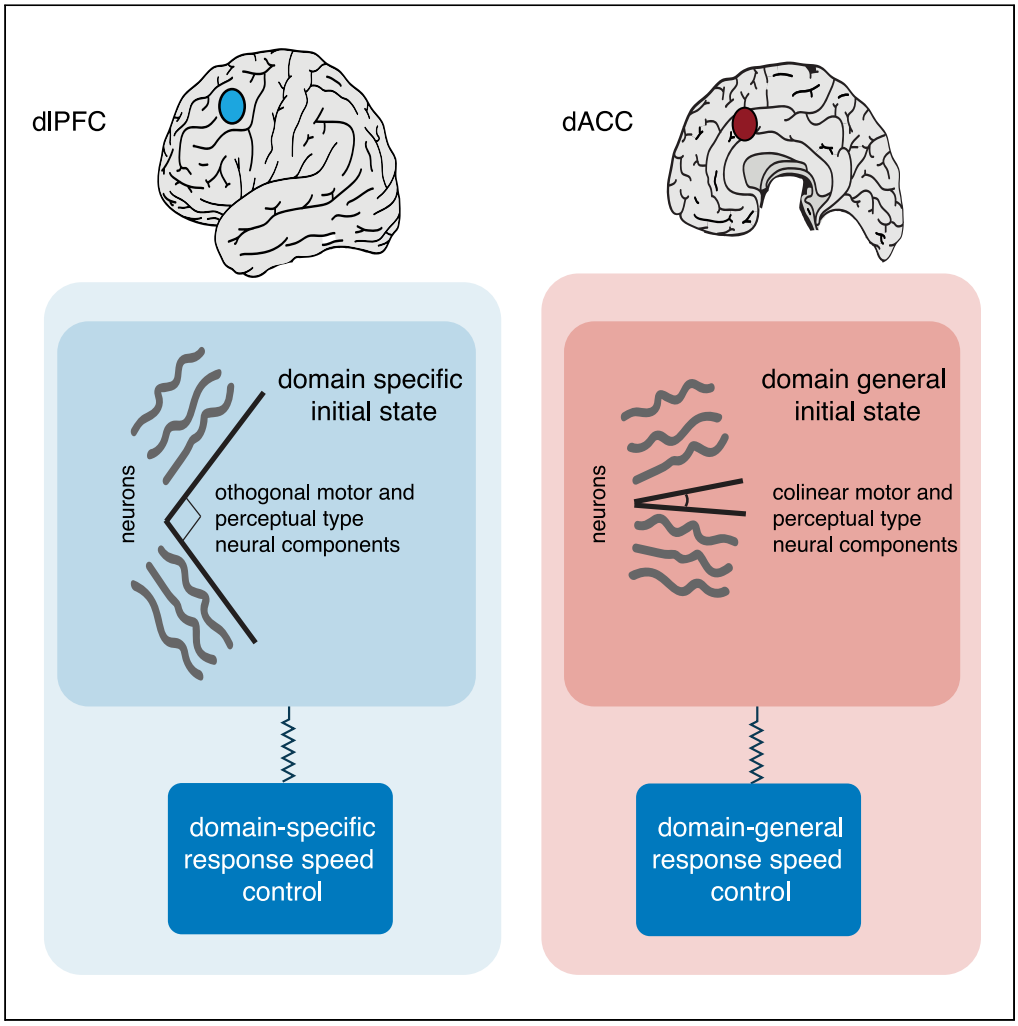

Alexander B. Herman, Elliot H. Smith, Catherine A. Schevon, ..., Matthew Botvinick, Benjamin Y. Hayden, Sameer A. Sheth

herma686@umn.edu

Highlights

dlPFC and dACC human neuron "initial state" firing patterns predicted response times

A domain-general initial state collapsed across conflict responses in dACC

In dlPFC, the initial state comprised domain-specific components

The dlPFC domain-specific components were oriented orthogonally

Herman et al., iScience 26, 108047
November 17, 2023
https://doi.org/10.1016/j.isci.2023.108047

iScience

CellPress
OPEN ACCESS

Article

Pretrial predictors of conflict response efficacy in the human prefrontal cortex

Alexander B. Herman,[1,10,*] Elliot H. Smith,[2,3] Catherine A. Schevon,[3] Mark J. Yates,[4] Guy M. McKhann,[4] Matthew Botvinick,[5] Benjamin Y. Hayden,[6,8,9] and Sameer A. Sheth[7,8,9]

SUMMARY

The ability to perform motor actions depends, in part, on the brain's initial state. We hypothesized that initial state dependence is a more general principle and applies to cognitive control. To test this idea, we examined human single units recorded from the dorsolateral prefrontal (dlPFC) cortex and dorsal anterior cingulate cortex (dACC) during a task that interleaves motor and perceptual conflict trials, the multisource interference task (MSIT). In both brain regions, variability in pre-trial firing rates predicted subsequent reaction time (RT) on conflict trials. In dlPFC, ensemble firing rate patterns suggested the existence of domain-specific initial states, while in dACC, firing patterns were more consistent with a domain-general initial state. The deployment of shared and independent factors that we observe for conflict resolution may allow for flexible and fast responses mediated by cognitive initial states. These results also support hypotheses that place dACC hierarchically earlier than dlPFC in proactive control.

INTRODUCTION

Our actions are determined by how stimulus-driven responses interact with ongoing neural activity.[1] In the motor system, one expression of this idea is the *initial state hypothesis*, which holds that motor control involves a series of dynamical states and that motor control requires a particular state.[2–7] Variability in performance, typically assessed with reaction times, corresponds partly to variability in pre-trial firing rates because those firing rate patterns reflect how close (or far) the brain's state is to the optimal response-driving initial state. We hypothesized that these principles might apply not just to motor systems but also to cognitive processes such as adaptive response to conflict. This hypothesis is motivated by recent theories that cognition can be seen as an extension of motor processing and that dynamical principles relevant to the motor system may apply to non-motor processes, including higher-level cognitive processes.[8–10] It is further motivated by evidence that responses to a stimulus can depend on the state of the brain even before stimulus onset.[4,11,12]

Conflict detection and resolution are a pair of complementary cognitive behaviors whose neuronal basis is beginning to be understood.[13–18] Conflict typically refers to a competition between possible stimuli for attention or action and generally evokes slower reaction times, increased error rates, and disengagement from alternative tasks.[19,20] When this refocusing of mental resources occurs in response to a conflict detection process, it is often referred to as *reactive control; proactive control*, on the other hand, refers to the pre-emptive deployment of mental resources to support conflict detection and resolution.[21–24] By analogy to the motor initial state hypothesis, we hypothesized that proactive control depends in part on variability in neural processes in conflict-relevant brain regions before the appearance of the conflict-inducing stimuli.[22,25]

Among conflict-responsive brain regions, the dorsal anterior cingulate cortex (dACC) and dorsolateral prefrontal cortex (dlPFC) are among the most studied brain regions.[16,18,26–28] Both regions are in the dorsal prefrontal cortex, showing systematic changes in hemodynamic response, local field potential (LFP), and firing rate in the presence of conflict (ibid.). dACC is most consistently implicated in sensing conflict during reactive control, while dlPFC has been observed to signal conflict demands during proactive control and, to a lesser extent, reactive control.[19,23,24,26,27,29] Consistent with this literature, we have recently proposed that these two regions play somewhat distinct, albeit complementary, roles in conflict detection and resolution during reactive control.[18] Specifically, we proposed that dACC is hierarchically earlier and thus carries a signal more akin to conflict detection and that dlPFC is more associated with implementation (see also[26,30]).

[1]Department of Psychiatry, University of Minnesota, Minneapolis, MN 55455, USA
[2]Department of Neurosurgery, University of Utah, Salt Lake City, UT 84132, USA
[3]Department of Neurology, Columbia University, NYC, NY 10027, USA
[4]Department of Neurological surgery, Columbia University, NYC, NY 10027, USA
[5]DeepMind, London, UK
[6]Department of Neuroscience, Center for Magnetic Resonance Research, and Center for Neural Engineering, University of Minnesota, Minneapolis, MN 55455, USA
[7]Department of Neurosurgery, Baylor College of Medicine, Houston, TX 77030, USA
[8]McNair Medical Institute, Baylor College of Medicine, Houston, TX 77030, USA
[9]These two authors contributed equally
[10]Lead contact
*Correspondence: herma686@umn.edu
https://doi.org/10.1016/j.isci.2023.108047

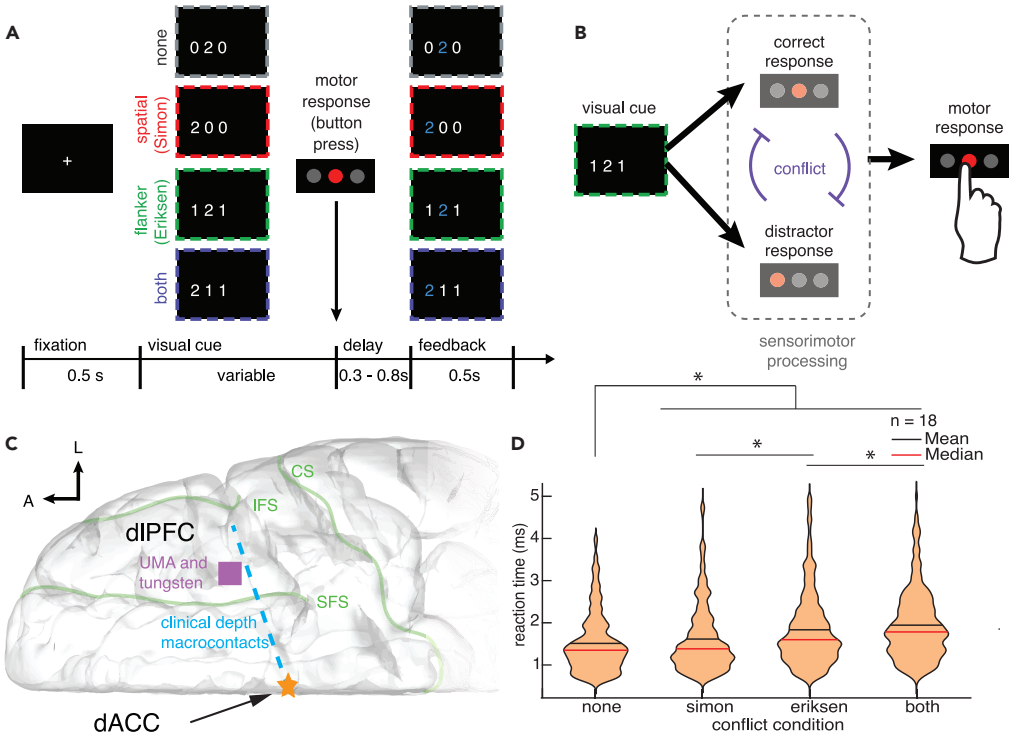

Figure 1. Multi-source interference task (MSIT) design, recording locations, and behavioral results

(A) Basic task design. Participants fixate on a central cross and then see a visual cue consisting of three numbers and must identify the unique number with a button push. The "correct response" is the left button if the target is 1, middle if 2, right if 3. Four example cues are shown here, and in each case, the target is "2" and the middle button is the correct response. This is most obvious for the first cue ("none"), where there is no conflicting information. In the other three examples, conflicting information makes the task more difficult. First, incongruence between the location of the target number in the 3-digit sequence and the location of the correct button in the 3-button pad produces spatial (Simon) conflict (orange). Second, the distracting presence of numbers that are valid button choices ("1," "2," and "3") produces flanker (Eriksen) conflict (green). Trials can also simultaneously have both types (blue).

(B) The visual cues are associated with one or more sensorimotor responses. Every cue has a correct response (the button press corresponding to the unique target). Cues can also have one or more distractor responses (the button press corresponding to task-irrelevant spatial information (Simon) or flanking distractors (Eriksen)). If and only if the correct and distractor responses do not match, then the cue causes conflict because only one button response can ultimately be chosen.

(C) Diagram of the intracranial implant including a stereotactically placed intra-cerebral depth electrode with clinical macroelectrodes (blue segments) along the shaft from dlPFC to dACC and microwire electrodes (orange star) in dACC. A, anterior; L, lateral; CS, central sulcus; SFS, superior frontal sulcus; IFS, inferior frontal sulcus. The UMA and tungsten microelectrode recording locations are schematized as a purple square on the surface of dlPFC.

(D) The average (mean) response times across participants in the four task conditions and (right) the mean response times within each participant. Bars = standard error across participants.

Here, we examined firing rates of single neurons in dACC and dlPFC during proactive and reactive control while humans performed the multi-source interference task (MSIT), a task that manipulates two different forms of conflict, a motor (Simon) type and a perceptual (Eriksen flanker) type.[31] In both regions, firing patterns before the trial (and before the presentation of the conflict-inducing stimuli) predicted the ability to resolve conflict in the upcoming trial; firing rate patterns in both regions after stimulus onset during reactive control also predicted conflict response times. During both the preparatory and response periods, the dACC appears to use a general code for conflict responding; the pattern of cell firing rates associated with better Simon performance also predicted better Eriksen performance. In dlPFC, by contrast, these codes were unrelated (orthogonal). Similarly, in dACC, the preparatory code was weakly related to the response code, while in dlPFC initial and response codes were orthogonal. Overall, these results endorse the idea that conflict resolution reflects the interaction between stimulus-driven reactive activity and ongoing fluctuations in proactive pre-trial activity, supports the initial state hypothesis for cognitive actions, and suggests distinct mechanisms in dACC and dlPFC with which the brain can respond both flexibly and efficiently to different conflict conditions.

RESULTS

Behavior

We examined responses of single neurons recorded in dACC and dlPFC in human patients undergoing intracranial monitoring for epilepsy or deep brain stimulation for movement disorders (Figure 1A). Task-related responses in subsets of this dataset were described in three earlier

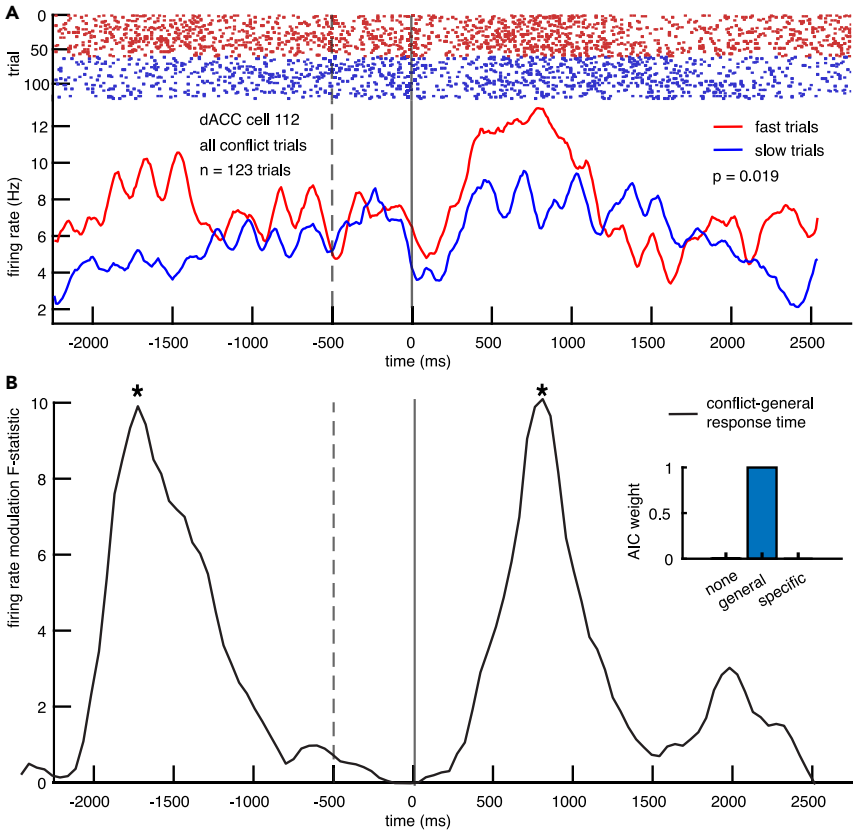

Figure 2. dACC neurons in the pre-trial period signal the speed of upcoming responses in a conflict-general manner

(A) PSTHs of example neuron 112 showing significantly higher pre-trial activity before fast (red) responses than slow (blue) responses across all conflict trial types (t-test on z-scored data). The dotted line indicates the start of fixation, and the solid vertical line indicates the stimulus onset.

(B) Time course of *F*-statistic for the area-level modulation of firing rate by conflict-general response time in dACC. Stars indicate the statistically significant peaks with highest *F*-value. Inset: Bar graph showing the AIC weight for three different models for response time encoding, showing that dACC area-level activity is best described by a conflict-general model.

studies, but pre-trial responses, the main focus of the present study, were not analyzed.[14,18,32] Participants performed the multi-source interference task (MSIT), a task that involves two independently manipulated types of conflict (Figure 1B). We collected data from 18 human participants. One group (dACC dataset) had 10 participants (all with epilepsy), while the other group (dlPFC dataset) had 8 participants (7 with Parkinson's Disease, 1 with epilepsy). One patient overlapped between the groups.

The validity of this task as a conflict manipulation has been demonstrated.[14,18,31,33] Therefore, we only briefly summarize the evidence that the task manipulates conflict. Most importantly, the median reaction time in the Simon trials (1.33 s) was significantly slower than no conflict trials (1.3 s, $p < 0.001$, $z = -13.7$, rank-sum = $1x10^9$). Likewise, reaction times in the Eriksen trials (1.55 s) were slower than in no-conflict trials ($p < 0.001$, $z = -53.6$, rank-sum = $1x10^9$) and Simon trials ($p < 0.001$, $z = -39.5$, ranksum = $1x10^9$. Finally, reaction times on both-conflict trials (1.73 s) were slower than on Simon trials ($p < 0.001$, $z = -62.4$, rank-sum = $19x10^8$) as well as compared to Eriksen: $p < 0.001$, $z = -25.2$, rank-sum = $1x10^9$). (Note that all differences survive Bonferroni correction).

Pre-trial single neuron correlates of conflict

We recorded from 138 neurons in dACC and 378 neurons in dlPFC. Our goal was to determine whether firing rate responses of neurons before the start of the trial predict subsequent reaction time. Consider, first, the firing rate responses of an example neuron shown in Figure 2, taken from dACC. Mean firing rates in the pre-trial period in this neuron were greater before faster reaction time trials than slower reaction time trials on trials for all conflict conditions (fast RT trials: 4.7 spikes/sec, slow RT trials 4 spikes/sec, $p = 0.0194$, t-test on z-scored data) and did not differ by conflict condition (Figure 2A). In our second example neuron, taken from dlPFC, mean firing rates were significantly greater before the start of faster reaction time trials than before slower reaction time trials in Eriksen-only but not Simon-only conditions (fast Eriksen RT trials: 1 spikes/sec, slow Eriksen RT trials: 0.5 spikes/sec, $p = 0.001$, t-test on z-scored data; fast Simon RT trials: 0.7 spikes/sec, slow Simon RT trials: 1.1 spikes/sec, $p = 0.18$, t-test on z-scored data, Figures 3A and 3B). Specifically, we ran a median split on reaction times post hoc

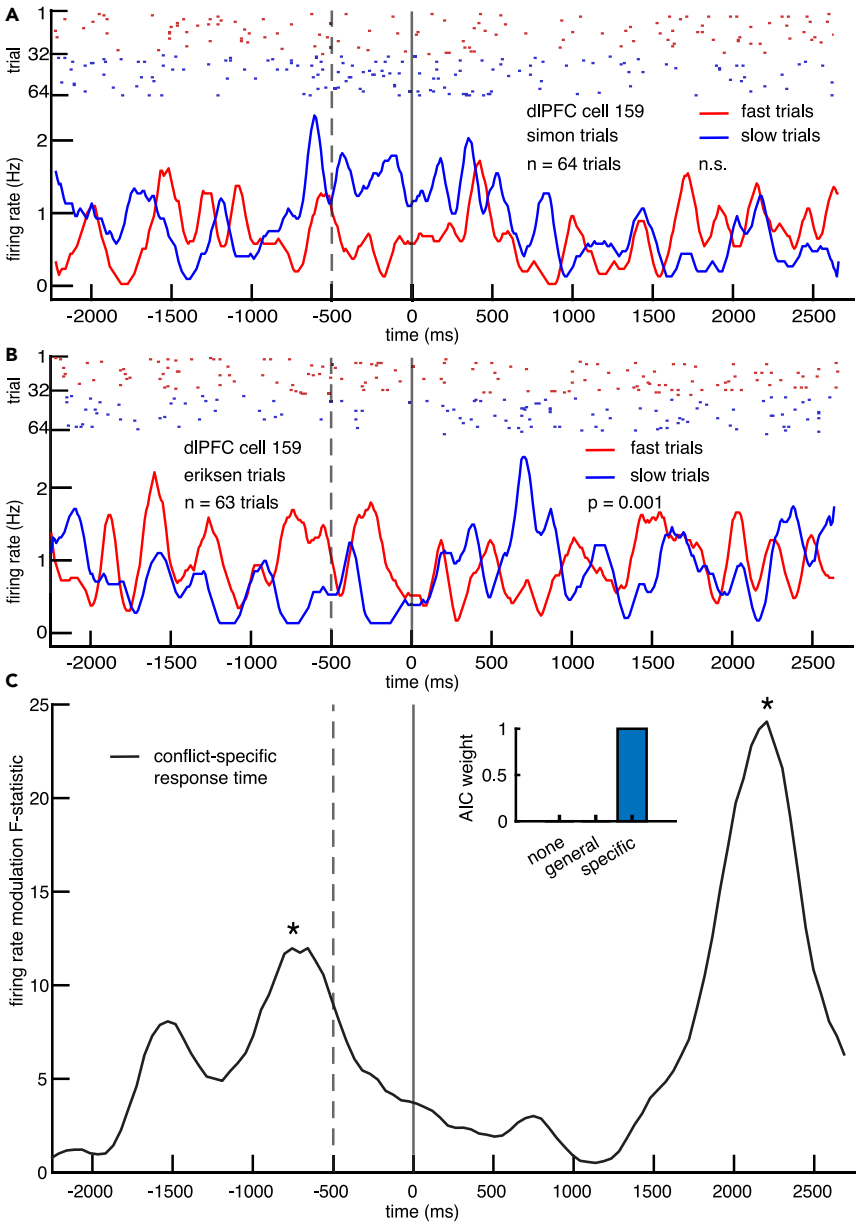

Figure 3. dlPFC neurons in the preparatory period signal the speed of upcoming responses in a conflict-specific manner

(A and B) PSTHs of example neuron 159 showing significantly higher pre-trial activity before fast (red) responses than slow (blue) responses in (b) Eriksen-only but not (a) Simon-only conflict trials (t-tests on z-scored data).

(C) Time course of *F*-statistics for the area-level modulation of firing rate by conflict-specific response time in dlPFC. Stars indicate the statistically significant peaks with highest *F*-value. Inset: Bar graph showing the AIC weight for three different models for response time encoding, showing that dlPFC area-level activity is best described by a conflict-specific model.

and separated firing rates on those two categories. (As described later in discussion, firing rates in these neurons also predicted the reaction time in a continuous model.).

Pre-trial population correlates of conflict

To explore these effects at the population level, we fit the spike count data within the entire pre-trial window for all neurons and all trials with a Poisson distribution generalized linear mixed-effects model (GLME) with patient number as a random effect and cell number as a random effect nested within patient.[34] Units with firing rates <0.1Hz over this period (22 dlPFC, 17 dACC) were excluded. Our analyses controlled for prior trial conflict type because conflict level on the previous trial can modulate preparatory neural responses and lead to trial-to-trial

adjustments, such as post-error slowing and conflict-adaptation/trial congruency effects (Horga et al., 2011; Sheth et al., 2012; Oehrn et al., 2014). Our analyses also controlled for previous trial reaction time (RT) to remove possible effects of slow drifts in arousal (Sklar et al., 2017). We estimated the dispersion for the Poisson distribution. We included participant and neuron as nested random effects to account for differences in contributions from single participants and single neurons to the group-level effects. All p values are reported as Bonferroni or false discovery rate (FDR) adjusted with the Benjamini-Hochberg method.[35] For each region, we compared three nested models: 1) a model with only a main effect for response time; 2) a model with an interaction term to capture conflict-general response time modulations in firing rate; and 3) a model with conflict-type specific interaction terms. For each area, we computed the Akaike Information Criterion weights for each of the three models and computed the weight ratio for each model, which ranges from 0 to 1 and reflects the evidence in support of that model relative to all other models considered.[36] The closer the weight ratio is to 1, the more that model is preferred over others. We found the conflict-general model to the dACC activity (Figure 2B inset, conflict-type general AIC weight 0.999), while the conflict-type specific model activity in dlPFC (Figure 3C inset, conflict-type specific AIC weight 0.997). Comparing the conflict-type general and specific models directly, we found that in dACC the conflict-general model was orders of magnitude more likely than the conflict-type specific model ($0.999/9 \times 10^{-43}$), and in dlPFC the conflict-type specific model was 300 times more likely than the conflict-type general model (0.997/0.003).

In dACC, examining the coefficients of the best fitting conflict-general model, we found that firing rate encoded variation in response time in the presence of any conflict (interaction, $F = 6.6$, DF = (1,30063), p = 0.036, Bonferroni-corrected permutation test). Previous trial reaction time and conflict did not significantly modulate the firing rate in dACC. In dlPFC, examining the best fitting conflict-specific model revealed that firing rate encoded overall response time at a trend level (main effect, $F = 4.3$, DF = 1, 1.08 × 10^5, Bonferroni corrected p = 0.051) and conflict-type specific response time significantly (interaction, $F = 13.5$, $DF = 2$, 1.08 × 10^, corrected $p < 0.001$). Previous trial reaction time and conflict condition modulated firing rate in dlPFC ($F = 20.0$, $DF = 2$, 1.08 × 10^5, Bonferroni corrected $p < 0.001$; $F = 5.1$, $DF = 1$, 1.08 × 10^5, Bonferroni corrected p = 0.052, permutation tests). We performed the same analysis on only correct trials, and the results were similar (dlPFC conflict-type $F = 13.1$, Bonferroni corrected $p < 0.001$, dACC conflict-general $F = 5.29$, Bonferroni corrected p = 0.017).

We next sought to determine whether response time encoding followed a dynamic, temporally specific time course in each brain area. We performed a sliding window GLME analysis for each area using the best-fitting model with 500 ms analysis windows and 100 ms steps. We FDR corrected the resulting p values across all time windows tested. In dACC, we found that pre-trial coding for conflict-general response time showed a clear peak at 1500 ms before stimulus onset (1000 ms before fixation cue onset) ($F = 10.97$, corrected $p < 0.001$, permutation test). In dlPFC, pre-trial coding for conflict-specific response time showed a clear peak at 750 ms before stimulus onset (250 ms before fixation cue onset) ($F = 12.2$, corrected p = 0.0016, permutation test, Figure 3C). In the response period, coding for conflict-general response time in dACC peaked at 1000 ms after stimulus onset ($F = 11.79$, corrected $p < 0.001$, permutation test, Figure 2B), while in dlPFC, coding for conflict-specific response time peaked at 2000 ms after stimulus onset ($F = 26.4$, corrected p = 0.0016, permutation test, Figure 3C).

We questioned whether pre-trial firing rates could predict upcoming reaction time and whether neuronal coding for firing rate prediction differed by conflict type, as suggested by the results above. We were specifically interested in whether such predictive coding of RT differed between conflict conditions on the single-cell level. To answer this question, we fit GLME models with reaction time as the dependent variable and included cell identity as a fixed effect. For dACC, we analyzed the peak time in the conflict-general model, while from dlPFC, we analyzed the peak coding time from the conflict-specific model. In dACC, we found that firing rate predicted reaction time in the presence of any conflict at the area level (conflict-general model, $F = 13.1$, $DF = 1$, 30215, corrected $p < 0.001$) and single-cell level ($F = 2.18$, $DF1 = 127$, $DF2 = 30215$, corrected $p < 0.001$). In dlPFC, we found that firing rate predicted reaction time for both Eriksen and Simon conditions at the area level ($F = 42.926$, $DF1 = 1$, $DF2 = 1.072e05$, corrected $p < 0.001$, $F = 6.89$, $DF1 = 1$, $DF2 = 1.072e05$, corrected p = 0.009) and exhibited highly significant single-cell effects for both conditions ($F = 1.49$, $DF1 = 355$, $DF2 = 1.072e05$, corrected $p < 0.001$, $F = 1.39$, $DF1 = 355$, $DF2 = 1.072e05$, corrected $p < 0.001$). These results indicate that pre-trial firing rates predict task performance, and that this predictive coding is more general in dACC yet stronger and more task-specific in dlPFC.

Orthogonal coding for two forms of conflict preparation in the dorsolateral prefrontal cortex

Having found that both *area* and *single-cell* activity in dlPFC contains conflict-type specific signals, we wondered if *population-level* activity in dlPFC might contain a conflict-type general signal. Here, we distinguish between area and population level as the difference between the group-level effect of firing rate on response time and the structure of single-cell firing rate coding in a population. To test this possibility, we asked how ensemble codes for predicting the resolution of Simon and Eriksen conflict, derived from the conflict-type specific model, were related. To do this, we calculated a vector of GLM regression weights for each distractor type across neurons. We call these vectors the *pre-trial tuning weight vectors*. We then compared these vectors by computing the angle between the Simon and Eriksen coefficients vectors. We tested these analyses on a pseudo-population of cells (n = 85) with significant coefficients for either conflict condition in the response or preparatory period, as well as on all cells, excluding cells with coefficients more than 4 absolute deviations from the median (n = 12 cells excluded); this approach allows us to include contributions from all relevant neurons, even those with real effects that do not pass the strict significance threshold for individual coefficients; this approach thus has better signal-to-noise (and is moderately less susceptible to Type II errors) than analyses that focus on cells that cross a significance threshold.[37] We found that in the conflict-significant population of dlPFC neurons, the angle θ between the codes for Simon and Eriksen is slightly greater than but not significantly different from 90° (θ = 98.4°, corrected p = 0.194, two-tailed permutation test; Figure 4A). This result is consistent with the orthogonal coding of the initial conditions that support proactive conflict resolution. In other words, the preparatory activity predisposing to fast responding to Simon conflict occurs along an axis orthogonal to Eriksen conflict. We found a similar result in the entire population, where θ was 93.8° and not significantly different

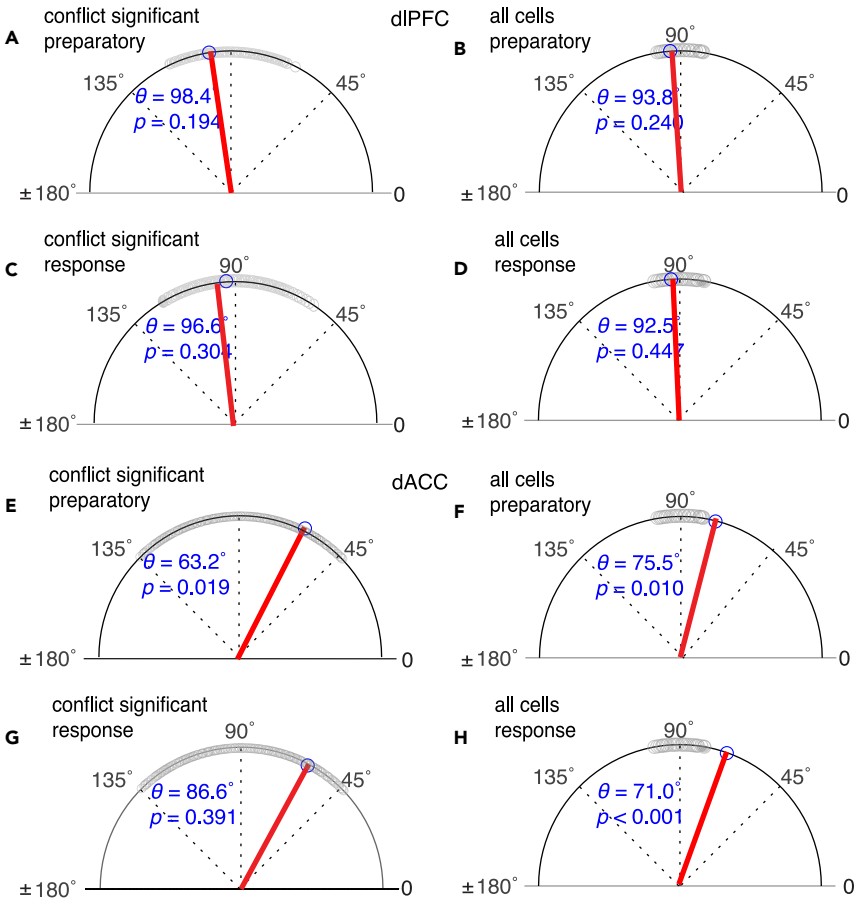

Figure 4. Orthogonal conflict-response coding in dlPFC and colinear coding in dACC. A 0° angle represents complete collinearity and 90° orthogonality

(A–D) the angle between Eriksen and Simon coding vectors in dlPFC, showing orthogonal coding (blue circle, blue numbering, and red line). The significance of the difference from a 90° (blue italics) was computed from permutation testing. The null distribution is shown with gray circles.

(E–H) The same but for dACC, showing colinear coding. p-values for all subpanels are calculated from two-tailed permutation tests.

from 90° (corrected p = 0.240, two-tailed permutation test). In the response period window, we again found orthogonal coding, with $\theta = 96.6°$ (corrected p = 0.304, two-tailed permutation test) for the conflict-significant population and 92.5° for all cells (corrected p = 0.447, two-tailed permutation test).

Partially co-linear coding for conflict in the dorsal anterior cingulate cortex

If dACC encodes conflict-responding in a domain-general fashion, as suggested by our model comparison results above, we expect to observe co-linearity between Eriksen and Simon coding vectors in a conflict-specific model, in contrast to dlPFC. To test this hypothesis, we performed a similar analysis as done for dlPFC, computing the angles between conflict-coding vectors. We found that Eriksen and Simon codes for all cells were partially co-linear in both the preparatory ($\theta = 63.2°$, corrected p = 0.019 two-tailed permutation test) and response periods ($\theta = 75.5°$, corrected p = 0.010, two-tailed permutation test), and for both conflict-significant and all cell populations in the response period ($\theta = 86.6°$, corrected p = 0.391 two-tailed permutation test; $\theta = 71°$, corrected $p < 0.001$ two-tailed permutation test, respectively).

To determine whether the angles from dACC differed from those from dlPFC, we compared the dACC angles to bootstrap distributions of angles from dlPFC. This is important to confirm because the difference between a significant and non-significant effect is not necessarily itself significant.[38] Confirming our hypothesis, we found the angles for both the conflict-significant and all cell populations differed significantly in the preparatory period (both corrected $p < 0.001$, one-tailed permutation tests), as well as the response period (corrected p = 0.049 and $p < 0.001$, respectively, one-tailed permutation test).

Preparatory and response period neural codes for reaction time in the dorsolateral prefrontal cortex are orthogonal

Lastly, we examined the degree to which the dlPFC preparatory state resembled the response state by computing similarity measures for their respective sets of coding vectors. We found that the pre-trial and response-tuning weight vectors were orthogonal in dlPFC and co-linear in

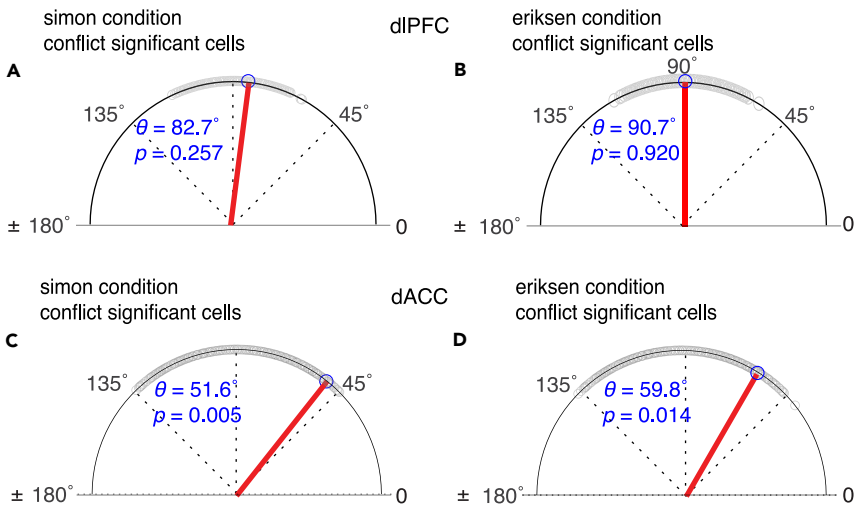

Figure 5. Orthogonality between preparatory and response conflict-response coding in dlPFC and partial collinearity in dACC

(A and B) A 0° angle represents complete collinearity and 90° orthogonality. Coding vector angles for significant cells in dlPFC for (a) Simon condition and (b) Eriksen condition.

(C and D) The same thing but for dACC. Legend is the same as for Figure 5. p-values for all subpanels are calculated from two-tailed permutation tests.

dACC (Figure 5). In dlPFC, the angle θ between Eriksen codes for conflict-preferring cells during the preparatory period was 88.1° and not significantly different from 0 (corrected p = 0.544, two-tailed permutation test, Figures 5A and 5B). It was 87.2° for the Simon condition and not significantly different from 0 (corrected p = 0.366, two-tailed permutation test). The codes for all cells were more aligned in the Simon condition (θ = 82°, corrected p = 0.014, two-tailed permutation test) but fully orthogonal in the Eriksen condition (θ = 88.1, corrected p = 0.520, two-tailed permutation test). In dACC (Figures 5C and 5D), we found a high level of co-linearity between preparatory and response codes in both the Simon (conflict-significant population θ = 50.6°, corrected p < 0.001; all cells θ = 61.6°, corrected p < 0.001; two-tailed permutation tests) and the Eriksen conditions (conflict-significant population θ = 66.9°, corrected p < 0.001; all cells θ = 72.4°, corrected p < 0.001; two-tailed permutation tests). The orthogonality of preparatory and response states in dlPFC and the co-linearity in dACC may suggest complementary mechanisms for minimizing interference between states while allowing for the efficiency of a shared representation.

DISCUSSION

We examined the responses of single neurons in human dACC and dlPFC during a task that interleaved and combined two kinds of conflict, Simon and Eriksen. We found that firing rates in both areas before the trial predict the efficacy of cognitive control, as inferred from reaction times. The fact that ensemble responses predict reaction time before the trial (and presumably before task-driven cognition) supports the hypothesis that successful cognitive control reflects, in part, the ability to transition through specific brain states. By controlling for prior trial condition and reaction time, we showed that these brain states do not simply reflect adaptation or drift in arousal but rather history-independent patterns predisposing to efficacious responding. Different models best described how dACC and dlPFC firing predicted upcoming conflict response. dACC activity was best described by a conflict-type general model, while dlPFC utilized a neural code specific for conflict-type. Moreover, the response predicting activity in dACC emerged before that in dlPFC, further implicating dACC as higher than dlPFC in a hierarchically organized brain system for conflict resolution.

Studies of motor control in rodents and non-human primates have shown that variability in the firing rates of neurons in motor cortex during movement preparation predicts variability in subsequent movements.[3,5,7] This body of work has given rise to the "initial state hypothesis," which posits that neural firing patterns behave as dynamical systems, and the trajectory of neural dynamics, therefore, depends on the initial state of the system.[4,6] One implication of this theory is that preparatory neural states can therefore be optimized to produce a desired behavioral outcome efficiently. If similar principles apply to neural dynamics during cognitive tasks, this suggests that preparatory activity may also be optimized to support the efficient application of cognitive control.

Indeed, a growing literature suggests neural patterns subserving cognition are also consistent with dynamical systems models.[39] It has been further proposed that cognitive performance may reflect a similar dynamical system view; however, this view has been difficult to test. We recently demonstrated that, in asynchronous choice, neurons in two core reward areas show subspace orthogonalization, a neural process previously associated only with the motor cortex.[40] Here we sought to test the hypothesis that the implementation of a cognitively controlled action would require the implementation of an initial state specific to the action. Our finding that ensemble patterns in dACC and dlPFC predict response speed supports the extension of the initial state hypothesis to cognitive control over behavior. Furthermore, the orthogonal initial states we observe in dlPFC for different types of conflict resolution suggest that they can be optimized for the performance of specific kinds of controlled behaviors.

These results have some bearing on the ongoing quest to understand the relationship between the dACC and dlPFC. These two regions are anatomically strongly interconnected, and both appear to play essential roles in higher cognition, but distinguishing their functions has proven difficult. We and others have proposed that they may be thought of as two stages along a hierarchy of control, with dACC being earlier than dlPFC in the hierarchy.[16,18,28,32] In this framework, dlPFC should be closer to control and dACC closer to detecting the need for control (i.e., conflict monitoring). These ideas are consistent with the idea that an earlier, general conflict signal would be found in dACC while a later implementation-specific initial state would be found in dlPFC. Speculatively, representations of task-relevant information may become more fully conflict-type specific and orthogonalized between dACC and dlPFC.[10] Here, we found evidence that the preparatory neural coding characterizing efficient responding may gain conflict-specificity between dACC and dlPFC. These findings thus shed light on *where* the essential neuronal computations that the human prefrontal cortex carries out to detect and resolve conflict to implement controlled behavior.

What are the implications of preparatory brain states for conflict resolution? One possibility is that initial states that predict response times reflect changes in arousal that are either spontaneous or the result of adaptations to the previous trial. While attractive for its simplicity, this explanation would not explain the persistence of the effect after controlling for trial history, nor would it explain the conflict type-specific nature of the initial states in dlPFC. Rather, our results suggest that the computations that perform conflict resolution are not only distinct, as implied by the divergent neural state space trajectories we found previously in this task[32], but are facilitated by shared and independent factors. In this task, participants do not have knowledge of whether the upcoming trial will have one form of conflict or the other or both. Maintaining shared and independent preparatory factors for conflict types in attentional states, independent of the past, may allow the brain to respond flexibly to unpredictable challenges while minimizing interference between the processes needed to respond to those challenges. Such a combination of shared and independent processes may also allow for optimizing the costs relative to the demands of cognitive control.[16] Why would preparatory states vary from trial to trial? The simplest explanation is spontaneous fluctuations due to noise. Another possibility is that participants or brain regions are making predictions, possibly subconsciously, about the demands of the upcoming trial, perhaps based on longer trial history than the recent past controlled for in this study.

Our results also touch on the notions of proactive and reactive control in the dual mechanisms of control theory.[21,22,25] According to this influential theory, the brain implements separate, independent processes for biasing (proactive) and shaping (reactive) responses to conflict. Proactive control is conceived of as either an extended goal or transient anticipatory state, while reactive control is a transient post-stimulus corrective response. Variability in the application of these control strategies is central to this theory. Our finding that both pre-trial and post-stimulus ensemble patterns predict conflict resolution in a recent history-independent manner and do so in an orthogonal fashion in dlPFC and a co-linear fashion in dACC is consistent with distinct proactive and reactive roles for these areas. The temporally specific patterns of activity we found are more consistent with a transient proactive state, reflecting the trial-to-trial nature of this task, which does not depend on the maintenance of temporally extended task contexts or goals.

Instead of imposing changes in task conditions and measuring differences in the resulting patterns of control as is often done, our design made use of natural trial-to-trial variability in response speed to infer control states. Whereas proactive and reactive control are typically conceptualized as task-amodal, we found evidence that they comprise domain-general and control-type specific components. The task-specific pre-trial coding we found in dlPFC relative to dACC is consistent with past results showing that dlPFC plays a more prominent role in proactive control.[24] Another important implication of our results is that proactive control may be implemented in part through the formation of initial states. Different forms of proactive control may drive neural activity in dlPFC into different initial states that bias toward efficient task-specific responding.

Conclusion

Our results suggest that not only does the initial state of neural activity before the cognitive act of conflict resolution support efficient responding in a pro-active manner, but it also does so through both conflict-general and conflict-type-specific mechanisms. It is intriguing to wonder if the collinearity we observe in dACC may contribute to untangling stimulus-action processes before full orthogonalization in dlPFC during implementation.[10] Previous work in premotor cortex has shown that the neural state space during responding predicts reaction times in motor tasks.[41] We found that these optimal initial states share some structure with the optimal responding states, suggesting they support optimal response trajectories. Future studies may examine whether initial states play a role in guiding how neural state-space trajectories may separate by response time differently depending on the specific cognitive computations the brain performs.

Limitations of the study

Our results must be interpreted considering significant limitations. Our study population consisted of people with epilepsy or Parkinson's Disease, so the generalization of our results to other populations remains speculative. Although we have controlled as much as possible for individual variability with the use of mixed-effects models, we are ultimately constrained by the small sample size of patients available for single-unit recordings and the variability of the number of neurons recorded from participants. Similarly, we lacked sufficient data to include a control area in our analysis. Lastly, although we found that dlPFC and dACC were better described by different models (conflict-response specific and conflict-response general, respectively) when we examined a single hierarchical model including both areas, we did not find a statistically significant difference between the conflict-coding in these areas. One possibility for this null result is that we lacked the power to detect a true difference; another is that although these areas are best fit by different models, the coefficients found by applying the same model are not different, two findings that are not mutually exclusive. Thus, the functional dissociation our results point to remains to be definitively established.

STAR★METHODS

Detailed methods are provided in the online version of this paper and include the following:

- KEY RESOURCES TABLE
- RESOURCE AVAILABILITY
  - Lead contact
  - Materials availability
  - Data and code availability
- EXPERIMENTAL MODEL AND STUDY PARTICIPANT DETAILS
- METHOD DETAILS
- QUANTIFICATION AND STATISTICAL ANALYSIS

SUPPLEMENTAL INFORMATION

Supplemental information can be found online at https://doi.org/10.1016/j.isci.2023.108047.

ACKNOWLEDGMENTS

This work was supported by NIH R01 MH106700, NIH U01 NS108923, NIH K12 NS080223, NIH S10 OD018211, NIH R01 NS084142, NIH R01 DA038615, NIH K23DA050909; the Brain and Behavior Foundation, and the Dana Foundation. Special thanks to Camilla Casadei, David K. Peprah, and Timothy G. Dyster for coordination and data collection efforts and R. Becket Ebitz for helpful discussions. The funders had no role in study design, data collection and analysis, decision to publish, or preparation of the article. Data were shared via a fully executed Data Use Agreement between Columbia University of Baylor College of Medicine.

AUTHOR CONTRIBUTIONS

SAS and MB designed the experiments, EHS, MHY and GMM conducted the experiments, ABH analyzed the data, and ABH, BYH and SAS wrote the paper.

DECLARATION OF INTERESTS

Dr. Sheth serves as a consultant for Boston Scientific, Zimmer Biomet, Neuropace, Koh Young, Varian Medical, Sensoria Therapeutics; and is a Co-founder of Motif Neurotech.

Received: February 18, 2022
Revised: July 14, 2023
Accepted: September 21, 2023
Published: September 27, 2023

REFERENCES

1. Pezzulo, G., and Cisek, P. (2016). Navigating the Affordance Landscape: Feedback Control as a Process Model of Behavior and Cognition. Trends Cogn. Sci. *20*, 414–424.
2. Riehle, A., and Requin, J. (1989). Monkey primary motor and premotor cortex: single-cell activity related to prior information about direction and extent of an intended movement. J. Neurophysiol. *61*, 534–549.
3. Churchland, M.M., Yu, B.M., Ryu, S.I., Santhanam, G., and Shenoy, K.V. (2006). Neural variability in premotor cortex provides a signature of motor preparation. J. Neurosci. *26*, 3697–3712.
4. Churchland, M.M., Cunningham, J.P., Kaufman, M.T., Ryu, S.I., and Shenoy, K.V. (2010). Cortical preparatory activity: representation of movement or first cog in a dynamical machine? Neuron *68*, 387–400.
5. Afshar, A., Santhanam, G., Yu, B.M., Ryu, S.I., Sahani, M., and Shenoy, K.V. (2011). Single-trial neural correlates of arm movement preparation. Neuron *71*, 555–564.
6. Shenoy, K.V., Sahani, M., and Churchland, M.M. (2013). Cortical control of arm movements: a dynamical systems perspective. Annu. Rev. Neurosci. *36*, 337–359.
7. Pandarinath, C., Ames, K.C., Russo, A.A., Farshchian, A., Miller, L.E., Dyer, E.L., and Kao, J.C. (2018). Latent Factors and Dynamics in Motor Cortex and Their Application to Brain-Machine Interfaces. J. Neurosci. *38*, 9390–9401.
8. Churchland, A.K., Kiani, R., and Shadlen, M.N. (2008). Decision-making with multiple alternatives. Nat. Neurosci. *11*, 693–702.
9. Pastor-Bernier, A., and Cisek, P. (2011). Neural Correlates of Biased Competition in Premotor Cortex. J. Neurosci. *31*, 7083–7088. https://doi.org/10.1523/jneurosci.5681-10.2011.
10. Yoo, S.B.M., and Hayden, B.Y. (2018). Economic Choice as an Untangling of Options into Actions. Neuron *99*, 434–447.
11. Weissman, D.H., Roberts, K.C., Visscher, K.M., and Woldorff, M.G. (2006). The neural bases of momentary lapses in attention. Nat. Neurosci. *9*, 971–978.
12. Boly, M., Balteau, E., Schnakers, C., Degueldre, C., Moonen, G., Luxen, A., Phillips, C., Peigneux, P., Maquet, P., and Laureys, S. (2007). Baseline brain activity fluctuations predict somatosensory perception in humans. Proc. Natl. Acad. Sci. USA *104*, 12187–12192.
13. Yeung, N., Holroyd, C.B., and Cohen, J.D. (2005). ERP correlates of feedback and reward processing in the presence and absence of response choice. Cereb. Cortex *15*, 535–544.
14. Sheth, S.A., Mian, M.K., Patel, S.R., Asaad, W.F., Williams, Z.M., Dougherty, D.D., Bush, G., and Eskandar, E.N. (2012). Human dorsal anterior cingulate cortex neurons mediate ongoing behavioural adaptation. Nature *488*, 218–221.
15. Ebitz, R.B., and Platt, M.L. (2015). Neuronal activity in primate dorsal anterior cingulate cortex signals task conflict and predicts adjustments in pupil-linked arousal. Neuron *85*, 628–640.
16. Shenhav, A., Musslick, S., Lieder, F., Kool, W., Griffiths, T.L., Cohen, J.D., and Botvinick, M.M. (2017). Toward a Rational and Mechanistic Account of Mental Effort. Annu. Rev. Neurosci. *40*, 99–124.
17. Bryden, D.W., Brockett, A.T., Blume, E., Heatley, K., Zhao, A., and Roesch, M.R. (2019).

Single Neurons in Anterior Cingulate Cortex Signal the Need to Change Action During Performance of a Stop-change Task that Induces Response Competition. Cereb. Cortex *29*, 1020–1031.

18. Smith, E.H., Horga, G., Yates, M.J., Mikell, C.B., Banks, G.P., Pathak, Y.J., Schevon, C.A., McKhann, G.M., 2nd, Hayden, B.Y., Botvinick, M.M., and Sheth, S.A. (2019). Widespread temporal coding of cognitive control in the human prefrontal cortex. Nat. Neurosci. *22*, 1883–1891.
19. Botvinick, M.M., Braver, T.S., Barch, D.M., Carter, C.S., and Cohen, J.D. (2001). Conflict monitoring and cognitive control. Psychol. Rev. *108*, 624–652.
20. Botvinick, M.M., and Cohen, J.D. (2014). The Computational and Neural Basis of Cognitive Control: Charted Territory and New Frontiers. Cogn. Sci. *38*, 1249–1285. https://doi.org/10.1111/cogs.12126.
21. Braver, T.S. (2012). The variable nature of cognitive control: a dual mechanisms framework. Trends Cogn. Sci. *16*, 106–113.
22. Stuphorn, V., and Emeric, E.E. (2012). Proactive and reactive control by the medial frontal cortex. Front. Neuroeng. *5*, 9.
23. Jiang, J., Beck, J., Heller, K., and Egner, T. (2015). An insula-frontostriatal network mediates flexible cognitive control by adaptively predicting changing control demands. Nat. Commun. *6*, 8165.
24. Braver, T.S., Kizhner, A., Tang, R., Freund, M.C., and Etzel, J.A. (2021). The Dual Mechanisms of Cognitive Control Project. J. Cogn. Neurosci. *1–26*.
25. Chen, X., Scangos, K.W., and Stuphorn, V. (2010). Supplementary motor area exerts proactive and reactive control of arm movements. J. Neurosci. *30*, 14657–14675.
26. MacDonald, A.W., 3rd, Cohen, J.D., Stenger, V.A., and Carter, C.S. (2000). Dissociating the role of the dorsolateral prefrontal and anterior cingulate cortex in cognitive control. Science *288*, 1835–1838.
27. Miller, E.K., and Cohen, J.D. (2001). An integrative theory of prefrontal cortex function. Annu. Rev. Neurosci. *24*, 167–202.
28. Shenhav, A., Botvinick, M.M., and Cohen, J.D. (2013). The expected value of control: an integrative theory of anterior cingulate cortex function. Neuron *79*, 217–240.
29. Kerns, J.G., Cohen, J.D., MacDonald, A.W., 3rd, Cho, R.Y., Stenger, V.A., and Carter, C.S. (2004). Anterior cingulate conflict monitoring and adjustments in control. Science *303*, 1023–1026.
30. Johnston, K., Levin, H.M., Koval, M.J., and Everling, S. (2007). Top-down control-signal dynamics in anterior cingulate and prefrontal cortex neurons following task switching. Neuron *53*, 453–462.
31. Bush, G., Shin, L.M., Holmes, J., Rosen, B.R., and Vogt, B.A. (2003). The Multi-Source Interference Task: validation study with fMRI in individual subjects. Mol. Psychiatry *8*, 60–70.
32. Ebitz, B.R., Smith, E.H., Horga, G., Schevon, C.A., Yates, M.J., McKhann, G.M., Botvinick, M.M., Sheth, S.A., and Hayden, B.Y. (2020). Human dorsal anterior cingulate neurons signal conflict by amplifying task-relevant information. Preprint at bioRxiv. https://doi.org/10.1101/2020.03.14.991745.
33. Deng, Y., Wang, X., Wang, Y., and Zhou, C. (2018). Neural correlates of interference resolution in the multi-source interference task: a meta-analysis of functional neuroimaging studies. Behav. Brain Funct. *14*, 8.
34. Yu, Z., Guindani, M., Grieco, S.F., Chen, L., Holmes, T.C., and Xu, X. (2022). Beyond t test and ANOVA: applications of mixed-effects models for more rigorous statistical analysis in neuroscience research. Neuron *110*, 21–35. https://doi.org/10.1016/j.neuron.2021.10.030.
35. Benjamini, Y., and Hochberg, Y. (1995). Controlling the False Discovery Rate: A Practical and Powerful Approach to Multiple Testing. J. Roy. Stat. Soc. B *57*, 289–300. https://doi.org/10.1111/j.2517-6161.1995.tb02031.x.
36. Wagenmakers, E.-J., and Farrell, S. (2004). AIC model selection using Akaike weights. Psychon. Bull. Rev. *11*, 192–196.
37. Blanchard, T.C., Hayden, B.Y., and Bromberg-Martin, E.S. (2015). Orbitofrontal cortex uses distinct codes for different choice attributes in decisions motivated by curiosity. Neuron *85*, 602–614.
38. Nieuwenhuis, S., Forstmann, B.U., and Wagenmakers, E.-J. (2011). Erroneous analyses of interactions in neuroscience: a problem of significance. Nat. Neurosci. *14*, 1105–1107.
39. Taghia, J., Cai, W., Ryali, S., Kochalka, J., Nicholas, J., Chen, T., and Menon, V. (2018). Uncovering hidden brain state dynamics that regulate performance and decision-making during cognition. Nat. Commun. *9*, 2505. https://doi.org/10.1038/s41467-018-04723-6.
40. Yoo, S.B.M., and Hayden, B.Y. (2020). The Transition from Evaluation to Selection Involves Neural Subspace Reorganization in Core Reward Regions. Neuron *105*, 712–724.e4.
41. Michaels, J.A., Dann, B., Intveld, R.W., and Scherberger, H. (2015). Predicting Reaction Time from the Neural State Space of the Premotor and Parietal Grasping Network. J. Neurosci. *35*, 11415–11432.
42. Widge, A.S., Zorowitz, S., Basu, I., Paulk, A.C., Cash, S.S., Eskandar, E.N., Deckersbach, T., Miller, E.K., and Dougherty, D.D. (2019). Deep brain stimulation of the internal capsule enhances human cognitive control and prefrontal cortex function. Nat. Commun. *10*, 1536.

STAR★METHODS

KEY RESOURCES TABLE

REAGENT or RESOURCE	SOURCE	IDENTIFIER
Software and algorithms		
fitGLME function for computing generalized linear mixed effect models	MATLAB, the Mathworks, Inc	
Psychtoolbox MATLAB functions for task administration	http://psychtoolbox.org/	
Offline Sorter (OLS) software	Plexon, Inc, Dallas, TX; USA	

RESOURCE AVAILABILITY

Lead contact

Alexander B. Herman (herma686@umn.edu).

Materials availability

No new reagents were generated in this study.

Data and code availability

- Data supporting the findings of this study are available from the lead contact upon request.
- Code supporting the findings of this study is available at https://github.com/abherman99/pretrial_RT_prediction.
- Any additional information required to reanalyze the data reported in this paper is available from the lead contact upon request.

EXPERIMENTAL MODEL AND STUDY PARTICIPANT DETAILS

We studied two cohorts of participants. Cohort 1 consisted of 9 patients (1 female) with medically refractory epilepsy who were undergoing intracranial monitoring to identify seizure onset regions. Before the start of the study, these participants were implanted with stereo-encephalography (sEEG) depth electrodes using standard stereotactic techniques. One or more of the sEEG electrodes in this cohort spanned dorsolateral prefrontal cortex (dlPFC) to dorsal anterior cingulate cortex (dACC; Brodmann's areas 24a/b/c and 32), as well as single unit recordings in dACC (see below; Data Acquisition).

Cohort 2 consisted of 8 patients: 7 (1 female) with movement disorders (Parkinson's disease or essential tremor) who were undergoing deep brain stimulation (DBS) surgery, and one male patient with epilepsy undergoing intracranial seizure monitoring. The entry point for the trajectory of the DBS electrode is typically in the inferior portion of the superior frontal gyrus or superior portion of the middle frontal gyrus, within 2 cm of the coronal suture. This area corresponds to dlPFC (Brodmann's areas 9 and 46). The single epilepsy patient in this cohort underwent a craniotomy for placement of subdural grid/strip electrodes in a prefrontal area including dlPFC and was implanted with a Utah-style microelectrode array (UMA) as part of a study on the neuronal dynamics of seizures.

All decisions regarding sEEG and DBS trajectories, craniotomy location, and microelectrode array position were made solely based on clinical criteria. The Columbia University Medical Center Institutional Review Board approved these experiments, and all participants provided informed consent prior to participating in the study.

METHOD DETAILS

All participants performed the multi-source interference task (MSIT; Figure 1A). In this task, each trial began with a 500-millisecond fixation period. This was followed by a cue indicating the ***correct response*** as well as the ***distractor response***. The cue consisted of three integers drawn from {0, 1, 2, 3}. One of these three numbers (the "***correct response cue***") was different from the other two numbers (the "***distractor response cues***"). Participants were instructed to indicate the identity of the correct response number on a 3-button pad. The three buttons on this pad corresponded to the numbers 1 (left button), 2 (middle) and 3 (right), respectively.

The MSIT task therefore presented two types of conflict. Simon (motor spatial) conflict occurred if the correct response cue was located in a different position in the cue than the corresponding position on the 3-button pad (e.g., '0 0 1'; target in right position, but left button is correct choice). Eriksen (flanker) conflict occurred if the distractor numbers were possible button choices (e.g., '3 2 3', in which "3" corresponds to a possible button choice; vs. '0 2 0', in which "0" does not correspond to a possible button choice).

After each participant registered his or her response, the cue disappeared, and feedback appeared. The feedback consisted of the target number, but it appeared in a different color. The duration of the feedback was variable (300 to 800 milliseconds, drawn from a uniform

distribution therein). The inter-trial interval (including the 500ms fixation/preparatory period) varied uniformly randomly between 1.5 and 2 seconds.

The task was presented on a computer monitor controlled by the Psychophysics MATLAB Toolbox (www.psychtoolbox.org; The MathWorks, Inc). This software interfaced with data acquisition cards (National Instruments,) that allowed for synchronization of behavioral events and neural data with sub-millisecond precision.

Single unit activity (SUA) was recorded from a combination of two techniques. The DBS surgeries were performed according to standard clinical procedure, using clinical microelectrode recording (Frederick Haer Corp.). Prior to inserting the guide tubes for the clinical recordings, we placed the microelectrodes in the cortex under direct vision to record from dlPFC, (IRB-AAAK2104). The epilepsy implant in Cohort 2 included a UMA implanted in dlPFC (IRB-AAAB6324). In all cases, data were amplified, high-pass filtered and digitized at 30 kilosamples per second on a neural signal processor (Blackrock Microsystems, LLC).

QUANTIFICATION AND STATISTICAL ANALYSIS

SUA data were re-thresholded offline at negative four times the root mean square of the 250 Hz high pass filtered signal. Well-isolated action potential waveforms were then segregated in a semi-supervised manner using the T-distribution expectation-maximization method on a feature space comprised of the first three principal components using Offline Sorter (OLS) software (Plexon Inc, Dallas, TX; USA). The times of threshold crossing for identified single units were retained for further analysis.

Single units with average firing rates < 0.1Hz during the 2-second pre-trial period were excluded from the analysis (22 dlPFC, 17 ACC).

We first fit gamma distributions to the reaction times and excluded reaction times with a less than 0.005 probability following.[42] For each model, we centered and scaled continuous predictor variables by z-scoring. We analyzed correct and incorrect trials to prevent false positives from data-censoring effects and performed confirmatory analyses on correct trials only, as noted. We conducted our initial analysis and model selection during the entire pre-trial period. We excluded neurons with firing rates < 0.1Hz over this period (22 dlPFC, 17 dACC). We fit generalized linear mixed effects models with the *fitglme* function in MATLAB, with total spike count in the 2s pretrial period as the response variable, reaction time, conflict, and their interaction, as well as previous trial conflict and reaction time, as the fixed effects, and participant ID and diagnosis as random intercepts, and cell ID as a random intercept nested within participant. We also examined a model with random slopes for the response time but for both dACC and dlPFC these models had worse model fits (higher AIC values). We compared three alternative models: a model with only a main effect of reaction time (RT)

$$FR_t \sim RT_t + RT_{t-1} + ConflictType_{t-1} + (1|SubjID) + (1|Cell1D : Subj1D)$$

a model with interaction term between RT and a binary variable for the presence of any kind of conflict (Eriksen, Simon or both)

$$FR_t \sim RT_t + RT_t + Conflict_t + Conflict_t + RT_{t-1} + Conflict_{t-1} + (1|SubjID) + (1|Cell1D : Subj1D)$$

and a model with an interaction term between RT and a categorical variable with different levels for different conflict types

$$FR_t \sim RT_t + RT_t : ConflictType_t + ConflictType_t + RT_{t-1} + ConflictType_{t-1} + (1|SubjID) + (1|Cell1D : Subj1D)$$

using Wilkinson notation, where FR is firing rate (here the spike count over the window) on all trials, *RT* is reaction time, *t* is the trial, *ConflictType* is a categorical variable with different levels for each type of conflict, and *Conflict* is a binary indicator variable for trials with any conflict, *SubjID* is the participant ID number and *CellID* is the cell number, with the syntax 1| indicating a random effect. We used a Poisson distribution for the firing rate (count over the specified window) and a log link function, and estimated the dispersion for the model from the data to allow for over or under-dispersion.[37] We also examined models with diagnosis (epilepsy or Parkinson's Disease) included as an additional random effect, but this produced no change in the model likelihoods. We compared these models by their AIC weights (Wagenmakers and Farrell, 2004). We identified the best fitting model as the model with the highest AIC weight ratio for all pairwise comparisons. To assess the magnitude and significance of fixed effects we performed ANOVA tests on the GLMEs with the MATLAB *ANOVA* function (McCullagh and Nelder, 2019) with alpha Bonferroni-adjusted for the number of fixed effects and computed *p*-values relative to a shuffled surrogate distribution.

We used the winning models from the whole-period analysis above for the sliding window-analysis and applied those models to 500ms windows sliding in steps of 25ms. For each step, we computed *p*-values relative to a shuffled surrogate distribution. We then FDR corrected all *p*-values across all time windows. The peak window for each area in both the pre-trial and response period was taken as the window with the highest (statistically significant) *F*-statistic from an ANOVA on the GLME coefficients.

For the reaction time prediction/decoding, we included Cell ID as a fixed effect to test for single-cell encoding and a group-level effect. We analyzed the peak time windows from the sliding-window analysis for pre-trial and response periods. Based on the results from the firing rate model, we utilized a conflict-type general model for dACC, with one coefficient = 1 for any type of conflict

$$RT_t \sim FR_t * \text{Cell1D} + FR_t * Conflict_t * \text{Cell1D} + Conflict_t + ConflictType_{t-1} + (1|SubjID)$$

and a model with separate, additive conflict terms for Simon and Eriksen conditions for dlPFC.

$$RT_t \sim FR_t * \text{Cell1D} + FR_t * EriksenTrials_t * Cell1D * EriksenTrials_t + FR_t * SimonTrials_t$$
$$* Cell1D + SimonTrials_t + ConflictType_{t-1} + (1|SubjID)$$

Here, we used a normal distribution with a log link function.

To compare the neural codes for conflict conditions, we fit individual GLM models to each neuron:

$$RT_t \sim FR_t + FR_t * ConflictType_t + ConflictType_t + RT_{t-1} + ConflictType_{t-1}$$

entered the model coefficients into individual vectors for each conflict condition. We computed the angle between the vectors as the inverse of the cosine similarity using the MATLAB formula

$$Ang = real\left(acosd\left(\max\left(\min\left(\frac{dot(B(:,1)-mean(B(:,1)),B(:,2)-mean(B(:,2)))}{norm(B(:,1)-mean(B(:,1)))*norm(B(L,2))}\right),1\right),-1\right)\right)$$

where B(:,1) is the first vector and B(:,2) is the second vector. We excluded points more than 4 median absolute deviations from the median, excluding 12 cells. We used non-parametric statistics because we did not in general, have enough data to characterize our data distributions fully. We randomized the vector entries and computed correlations between the randomized vectors to form null distributions (2000 permutations). We computed p-values for the real measurement relative to the corresponding null distribution (permutation test). To compare angles and correlations, we constructed bootstrap distributions with resampling (5000 samples) and compared the medians of the resultant distributions to the measured angle in the other condition with the non-parametric Wilcoxon rank sum test.